CT理论与应用研究
Computerized Tomography Theory and Applications

基于MRI T2加权成像纹理分析评估青少年脊柱侧弯患者椎间盘退变的可行性研究

王凤仙，王守丰，常 莹，周 晋，陈 静，周正扬，王冬梅

The Feasibility of Texture-based Quantification for Evaluating Lumbar Intervertebral Disc Degeneration in Adolescent Idiopathic Scoliosis from Conventional T2-weighted Magnetic Resonance Imaging

WANG Fengxian, WANG Shoufeng, CHANG Ying, ZHOU Jin, CHEN Jing, ZHOU Zhengyang, and WANG Dongmei

在线阅读 View online: https://doi.org/10.15953/j.ctta.2022.225

王凤仙, 王守丰, 常莹, 等. 基于 MRI T2 加权成像纹理分析评估青少年脊柱侧弯患者椎间盘退变的可行性研究[J]. CT 理论与应用研究, 2023, 32(6): 735-745. DOI:10.15953/j.ctta.2022.225.（英）.
WANG F X, WANG S F, CHANG Y, et al. The Feasibility of Texture-based Quantification for Evaluating Lumbar Intervertebral Disc Degeneration in Adolescent Idiopathic Scoliosis from Conventional T2-weighted Magnetic Resonance Imaging[J]. CT Theory and Applications, 2023, 32(6): 735-745. DOI:10.15953/j.ctta.2022.225.

The Feasibility of Texture-based Quantification for Evaluating Lumbar Intervertebral Disc Degeneration in Adolescent Idiopathic Scoliosis from Conventional T2-weighted Magnetic Resonance Imaging

WANG Fengxian[a], WANG Shoufeng[b], CHANG Ying[a], ZHOU Jin[a], CHEN Jing[a], ZHOU Zhengyang[a]✉, WANG Dongmei[2]✉

1. a). Department of Radiology; b). Department of Orthopedic Surgery, Nanjing Drum Tower Hospital, The Affiliated Hospital of Nanjing University Medical School, Nanjing 210008, China
2. Department of Radiology, Shanghai Municipal Hospital of Traditional Chinese Medicine, Shanghai University of Traditional Chinese Medicine, Shanghai 200071, China

Abstract: Objective: To investigate the utility of texture data based on T2-weighted magnetic resonance imaging (MRI) in determining intervertebral disc degeneration in adolescent idiopathic scoliosis (AIS). Materials and Methods： From October 2016 and March 2020, 122 patients with AIS and 40 volunteers who underwent 3.0T MRI were prospectively included. The following MRI texture data were generated: (1) mean, (2) standard deviation, (3) max, (4) min, (5) the fifth, 10th, 25th, 50th, 75th and 90th percentiles; (6) skewness; (7) kurtosis; and (8) entropy. The Pfirrmann system was used to evaluate the intervertebral discs of all participants. Patients with Pm I were divided into groups 1 and 2. Volunteers were classified into 0. Differences and correlations between the groups were analyzed. Results: The mean, standard deviation, max, entropy and the 5th, 10th, 25th, 50th, 75th, and 90th percentiles in group 2 were significantly lower than those in group 1 and group 0; the min in group 2 was significantly lower than in group 0; the skewness in group 2 was significantly higher than in group 1 and group 0; the kurtosis in group 2 was significantly lower than in group 1; the skewness in group 1 was significantly higher than in group 0 and the standard deviation, min, kurtosis and 5th, 10th, 25th, and 50th percentiles in group 1 were significantly lower than those in group 0. Conclusion: Texture analysis can be used to assess early degenerative changes in the intervertebral discs of patients with AIS.

Keywords: MRI; texture analysis; adolescent idiopathic scoliosis; intervertebral disc degeneration

DOI:10.15953/j.ctta.2022.225 **CLC number**：R 445.2 **Documeng code**：A

1 Introduction

Adolescent idiopathic scoliosis (AIS) is the most common form of scoliosis developed in adolescents and can lead to intervertebral disc degeneration[1-3]. Magnetic resonance imaging (MRI) is currently the most important method for the clinical evaluation of intervertebral disc pathology as degenerative changes in the intervertebral discs can manifest as signal changes on T2-weighted MRI[4-5]. Therefore, MRI is widely used to evaluate the degeneration of intervertebral discs.

The currently recognized disc degeneration assessment system is the Pfirrmann grading system, which is based on MRI of the disc structure[4]. However, this method is limited for the detection of early

收稿日期：2022-11-14。
基金项目：江苏省六大人才高峰项目（2015-WSN-079）；南京市医学科技发展基金重点项目和南京市医学杰出青年人才项目（YKK15067；QRX11178）；江苏省重点医学青年人才、江苏省“十三五”健康促进工程（QNRC2016041）；南京医学科技发展基金（YKK17099）。

intervertebral disc degeneration and changes in the microstructure of the degenerated intervertebral disc, and as a qualitative-type analysis is prone to subjectivity. In addition, with the development of emerging treatment technologies such as cell[6] and growth factor therapy[7], it is important to quantitatively evaluate intervertebral disc degeneration and its efficacy.

Although a variety of functional imaging technologies have emerged to quantitatively evaluate changes in the microstructure of intervertebral discs (such as diffusion weighted (DW) imaging[8-9]), scan time has increased with the development of imaging technology. In addition, the parameters provided are limited and cannot be routinely performed and used in clinical settings, restricting clinical promotion capabilities and applications. Texture analysis refers to a variety of mathematical methods used to evaluate the grey-level intensity and position of pixels within an image to derive parameters automatically. It can not only provide quantitative parameters to reflect changes in the microstructure of the tissue, but also reflect the overall condition of the entire lesion and describe the local and regional relationships among the pixels in the region of interest (ROIs) to better reflect the heterogeneity of the organization[10]. Because of these advantages, texture parameters derived from MRI have been widely used as tools for viewing various diseases, especially in tumor imaging[11].

Our purpose was to obtain intervertebral disc texture data based on conventional T2 MRI for texture analysis and evaluate intervertebral disc degeneration in patients with AIS.

2 Material and methods

2.1 Subjects

This study was approved by our Institutional Ethics Committee. Informed consent was obtained from all participants after explaining the risks involved and the purpose of the study.

From October 2016 to March 2020, 122 consecutive patients with AIS were included in this trial. The inclusion criteria for patients were as follows: (1) adolescence (ages, 10- to 18-years-old); (2) preliminary diagnosis of idiopathic scoliosis based on a clinical examination and typical standing full-length radiographs[1,12]; (3) major thoracolumbar scoliotic curve; (4) no history of spinal surgery, spinal bracing treatment, or spinal trauma; and (5) ability to complete spine radiology examinations. Clinical and medication histories were collected from patients and their caretakers.

Forty matched healthy volunteers were recruited as group 0. The inclusion criteria were as follows: (1) age of 10~18 years; (2) no history of spinal trauma, back pain, or spinal surgery; and (3) complete radiography and MRI examinations without spinal abnormalities.

The Cobb angles were generated by determining and measuring the curve apex using the Cobb method on standard spinal radiographs[1,13]. The curved apexes of patients were located at T12 to L1; the average Cobb angle was (40.00 ± 13.62) degrees (range, 15~77 degrees).

2.2 Magnetic Resonance Examination

All MR scans were performed using a 3.0T MR system (Ingenia; Philips Healthcare, Best, Netherlands) with a 16-channel phased-array sensitivity-encoding abdominal coil and a 16-channel torso phased-array body coil. The MRI sequence used a segmented whole-spine scan, a parallel imaging technique, and partial Fourier acquisition (sense = yes, P reduction (AP) = 1.6, half-scan factor = 0.624), and the lumbar spine was scanned in an oblique sagittal position. The standard MR scan remained the same throughout the study: oblique sagittal images of T1-weighted turbo spin echo (TSE) sequence (repetition time (TR) = 450 ms, echo time (TE) = 16 ms, field of view (FOV) = 350 mm, matrix size = 264 × 389, voxel size = 0.7 × 0.9 × 3, slice thickness = 3 mm, intersection gap = 1 mm, echo trains = 1, turbo factor = 7); oblique sagittal images of T2-weighted TSE sequence (TR = 2800 ms, TE = 100 ms, FOV = 350 mm, matrix size = 204 × 340, voxel size = 0.9 × 1.04 × 3, slice thickness = 3 mm, intersection gap = 1 mm, echo trains = 1, turbo factor = 29); coronal T2-weighted TSE sequence (TR = 2800 ms, TE = 100 ms, FOV = 350 mm, matrix size = 204 × 340,

voxel size = 0.9 × 1.04 × 3 mm, slice thickness = 3 mm, intersection gap = 1 mm, echo trains = 1, turbo factor = 29). The MR scan lasted for 8 min and 53 s.

2.3 Imaging Analyses

Image analysis was independently performed by two staff radiologists with different levels of experience (W.F.X and W.D.M with 4 years and 15 years of experience in spine imaging, respectively); neither radiologist had knowledge of the clinical data of the patients. According to the Pfirrmann system[4], which is based on the MRI-evaluated disc structure and includes signal intensity and the distinction between nucleus, disc height, and annulus, two observers evaluated the intervertebral discs (including L3/4, L4/5, and L5/S1) of 122 AIS patients and 40 volunteers. The interverbal discs of all volunteers were Pm I, classified as group 0 (healthy control group) (12 males and 28 females; mean age, (15.05 ± 2.09) years; range, 11 ~ 18 years). For AIS patients, the Pfirrmann grade[4] is assigned based on the evaluation of the intervertebral discs (including L3/4, L4/5, and L5/S1) (previous studies found that lower intervertebral discs generally undergo early degeneration[14-15]). AIS patients with Pm I grade were divided into group 1 (AIS patients without obvious degeneration on MRI) (30 males and 64 females; mean age, (14.12 ± 1.90) years; age range, 11~17 years), and Pm II to V grades were classified into group 2 (AIS patients with degeneration on MRI) (12 males and 16 females; average age, (15.17 ± 2.19) years; age range, 11~18 years).

Texture analysis was performed on all participants using an internal software (Image Analyzer 2.0, Nanjing, China), as described in our previous studies[16-17]. After downloading patient images and transferring them to our internal software, we were able to manually sketch the regions of interest (ROIs) on the patients' images. After selecting all ROIs, the volume of interest (VOI) was determined. The software then automatically generated texture features. In all participants, at least two consecutive levels of the intervertebral disc nucleus pulposus (including L3/4, L4/5 and L5/S1) were selected to draw slice-by-slice the ROI and obtain the VOI. The average ROI area was 262.78 mm^2 (range, 99.99 ~ 589.75 mm^2) and the average VOI was 1 166.42 mm^3 (range, 439.97 ~ 2 874.02 mm^3).

The value of each pixel on the VOI was automatically measured to generate the following histogram features: (1) mean (mean T2 relaxation time); (2) standard deviation (dispersion of a frequency distribution); (3) max (maximum T2 relaxation time); (4) min (minimum T2 relaxation time); (5) the 5th, 10th, 25th, 50th, 75th, and 90th percentiles (cumulative nth percentile of T2 relaxation time histogram); (6) skewness (degree of histogram asymmetry around the mean); (7) kurtosis (statistics on the sharpness of the histogram peak); and (8) entropy (the degree of disorder of T2 relaxation time over the VOI). All images were independently analyzed by two radiologists. In addition to the interobserver agreement analysis, the mean of the values determined by the two radiologists were calculated for statistical analyses.

2.4 Statistical Analysis

MedCalc Statistical Software v.15.2.2 (MedCalc Software, Ostend, Belgium; http://www.medcalc.org; 2015) was used for receiver operating characteristic (ROC) analysis, and SPSS software 18.0, was used for all other statistical analyses. The intraclass correlation coefficient (ICC) was used to estimate the intra- and interobserver agreements of the parameter measurements (poor = 0.000 ~ 0.200, fair = 0.201 ~ 0.400, moderate = 0.301 ~ 0.600, good = 0.601 ~ 0.800, and excellent = 0.801 ~ 1.000). As most texture parameters did not have a normal distribution, a non-parametric test was used. The Kruskal-Wallis one-way ANOVA (K sample) test was used to compare the differences for all parameters among the three groups. The Spearman correlation coefficient©) was used to evaluate the trends of texture analysis parameters among the three groups (no correlation = 0.0 ~ 0.2, weak = 0.2 ~ 0.4, moderate = 0.4 ~ 0.6, strong = 0.6 ~ 0.8, and very strong = 0.8 ~ 1.0). ROC analysis (including the area under the ROC curve [AUC]) was used to evaluate the effectiveness of histogram-derived parameters for distinguishing participants among the three groups and to select cut-off values by calculating the maximal Youden index (Youden index = sensitivity + specificity – 1).

$P < 0.05$ was considered statistically significant.

3 Results

3.1 Kruskal-Wallis one-way ANOVA (K sample) test

The mean, standard deviation, max, entropy, and the 5th, 10th, 25th, 50th, 75th, and 90th percentiles in group 2 were significantly lower than those in group 1 and group 0; the min in group 2 was significantly lower than that in group 0; the skewness in group 2 was significantly higher than those in group 1 and group 0; the kurtosis in group 2 was significantly lower than that in group 1; the skewness in group 1 was significantly higher than those in group 0 and the standard deviation, min, kurtosis and 5th, 10th, 25th, and 50th percentiles in group 1 were significantly lower than those in group 0 (Fig.1, Tables 1 ~3).

Table 1 Kruskal-Wallis one-way ANOVA (K sample) test between group 0 and group 1

Paramter	Group		*P*
	0	1	
mean	202.103 ± 74.038	180.604 ± 47.484	1.000
standard-deviation	62.857 ± 22.634	77.961 ± 25.300	0.012*
min	28.325 ± 18.993	9.819 ± 6.796	< 0.001*
max	301.825 ± 97.987	326.010 ± 97.248	0.336
5th percentile	86.000 ± 32.214	48.521 ± 18.381	< 0.001*
10th percentile	106.150 ± 36.778	68.202 ± 23.571	< 0.001*
25th percentile	156.250 ± 61.812	116.617 ± 35.037	0.001*
50th percentile	217.700 ± 84.736	190.276 ± 51.065	0.450*
75th percentile	249.500 ± 88.844	246.914 ± 67.077	1.000
90th percentile	272.250 ± 93.633	275.617 ± 77.267	1.000
skewness	−0.538 ± 0.246	−0.324 ± 0.302	0.004*
kurtosis	2.470 ± 0.456	2.080 ± 0.335	< 0.001*
entropy	5.264 ± 0.216	5.410 ± 0.354	0.136

NOTE: Mean and percentile values are in units of ms. Mean = mean T2 relaxation time; standard deviation = spread of distribution; min = minimum T2 relaxation time; max = maximum T2 relaxation time; the 5th, 10th, 25th, 50th, 75th, and 90th percentiles = *n*th percentile T2 relaxation time of a cumulative histogram; skewness = histogram asymmetry degree around the mean; kurtosis = measurement of the histogram sharpness; entropy = the distribution of T2 relaxation time levels over the ROI. *−Statistically significant. $P < 0.05$ was considered statistically significant in differentiating the groups 0~1.

3.2 ROC Analysis

ROC analysis indicated that standard deviation, min, 5th percentile, 10th percentile, 25th percentile, skewness, kurtosis, and entropy differentiated between group 0 and group 1 (all $P < 0.05$), with an AUC of 0.637 ~ 0.865. The 5th percentile had the highest diagnostic efficiency in differentiating between the two groups and performed better than the standard deviation, 25th percentile, skewness, kurtosis, and entropy. With a cut-off value of 61 ms, the sensitivity and specificity of the 5th percentile in differentiating group 0 and group 1 were 0.734 and 0.900, respectively (AUC = 0.865).

ROC analysis indicated that the mean, standard deviation, min, max, skewness, entropy, and 5th, 10th, 25th, 50th, 75th, and 90th percentiles could differentiate between group 0 and group 2, with an AUC of 0.809 ~ 0.967. The 50th percentile had the highest diagnostic efficiency in differentiating between these two groups and performed better than min. With a cut-off value of 142 ms, the sensitivity and specificity of the 50th percentile in differentiating group 0 and group 1 were 0.964 and 0.950, respectively (AUC = 0.967).

ROC analysis indicated that the mean, standard deviation, min, max, skewness, kurtosis, entropy, and 5th, 10th, 25th, 50th, 75th, and 90th percentiles could differentiate between group 1 and group 2, with an

AUC of 0.634 ~ 0.960 ($P < 0.001 \sim 0.042$). The 50th percentile had the highest diagnostic efficiency in differentiating between the two groups and performed better than the 5th and 10th percentiles for skewness and kurtosis. With a cut-off value of 127 ms, the sensitivity and specificity of the 50th percentile in differentiating group 0 and group 1 were 0.893 and 0.957, respectively (AUC = 0.960) (Table 4).

Table 2　Kruskal-Wallis one-way ANOVA (K sample) test between group 0 and group 2

Paramter	Group		*P*
	0	2	
mean	202.103 ± 74.038	78.691 ± 44.100	< 0.001*
standard-deviation	62.857 ± 22.634	34.065 ± 16.268	< 0.001*
min	28.325 ± 18.993	11.142 ± 17.504	< 0.001*
max	301.825 ± 97.987	163.821 ± 71.492	< 0.001*
5th percentile	86.000 ± 32.214	29.178 ± 28.686	< 0.001*
10th percentile	106.150 ± 36.778	36.178 ± 31.232	< 0.001*
25th percentile	156.250 ± 61.812	51.928 ± 38.613	< 0.001*
50th percentile	217.700 ± 84.736	75.357 ± 44.333	< 0.001*
75th percentile	249.500 ± 88.844	103.892 ± 53.918	< 0.001*
90th percentile	272.250 ± 93.633	126.500 ± 62.421	< 0.001*
skewness	−0.538 ± 0.246	0.233 ± 0.406	< 0.001*
kurtosis	2.470 ± 0.456	2.499 ± 0.552	1.000
entropy	5.264 ± 0.216	4.636 ± 0.313	< 0.001*

NOTE: mean and all percentile values are in units of ms. Mean = mean T2 relaxation time; standard deviation = spread of distribution; min = minimum T2 relaxation time; max = maximum T2 relaxation time;the 5th, 10th, 25th, 50th, 75th, and 90th percentiles = *n*th percentile T2 relaxation time of a cumulative histogram; skewness = histogram asymmetry degree aroundthe mean; kurtosis = measurement ofthe histogram sharpness; entropy = the distribution of T2 relaxation time levels overthe ROI. *−Statistically significant. $P < 0.05$ was considered statistically significant in differentiatingthe group 0~2.

Table 3　Kruskal-Wallis one-way ANOVA (K sample) test between group 1 and group 2

Paramter	Group		*P*
	1	2	
mean	180.604 ± 47.484	78.691 ± 44.100	< 0.001*
standard-deviation	77.961 ± 25.300	34.065 ± 16.268	< 0.001*
min	9.819 ± 6.796	11.142 ± 17.504	0.280
max	326.010 ± 97.248	163.821 ± 71.492	< 0.001*
5th percentile	48.521 ± 18.381	29.1785 ± 28.686	< 0.001*
10th percentile	68.202 ± 23.571	36.178 ± 31.232	< 0.001*
25th percentile	116.617 ± 35.037	51.928 ± 38.613	< 0.001*
50th percentile	190.276 ± 51.065	75.357 ± 44.333	< 0.001*
75th percentile	246.914 ± 67.077	103.892 ± 53.918	< 0.001*
90th percentile	275.617 ± 77.267	126.5 ± 62.421	< 0.001*
skewness	−0.324 ± 0.302	0.233 ± 0.406	< 0.001*
kurtosis	2.080 ± 0.335	2.499 ± 0.552	< 0.001*
entropy	5.410 ± 0.354	4.636 ± 0.313	< 0.001*

NOTE: Mean and all percentile values are in units of ms. Mean = mean T2 relaxation time; standard deviation = spread of distribution; min = minimum T2 relaxation time; max = maximum T2 relaxation time;the 5th, 10th, 25th, 50th, 75th, and 90th percentiles = *n*th percentile T2 relaxation time of a cumulative histogram; skewness = histogram asymmetry degree aroundthe mean; kurtosis = measurement ofthe histogram sharpness; entropy = the distribution of T2 relaxation time levels overthe ROI. *−Statistically significant. $P < 0.05$ was considered statistically significant in differentiatingthe group 1~2.

3.3　The Spearman Correlation Coefficient

The Spearman correlation test indicated that the mean, standard deviation, min, max, the 5th, 10th, 25th,

50th, 75th, and 90th percentiles and the absolute value of skewness, kurtosis, and entropy correlated negatively from group 0 to group 2 ($r = -0.472$, $P < 0.001$; $r = -0.253$, $P = 0.001$; $r = -0.448$, $P < 0.001$; $r = -0.323$, $P < 0.001$; $r = -0.665$, $P < 0.001$; $r = -0.652$, $P < 0.001$; $r = -0.610$, $P < 0.001$; $r = -0.524$; $P < 0.001$; $r = -0.405$, $P < 0.001$; $r = -0.384$, $P < 0.001$; $r = -0.228$, $P = 0.003$; $r = -0.070$, $P = 0.379$; $r = -0.325$, $P < 0.001$) (Fig.2).

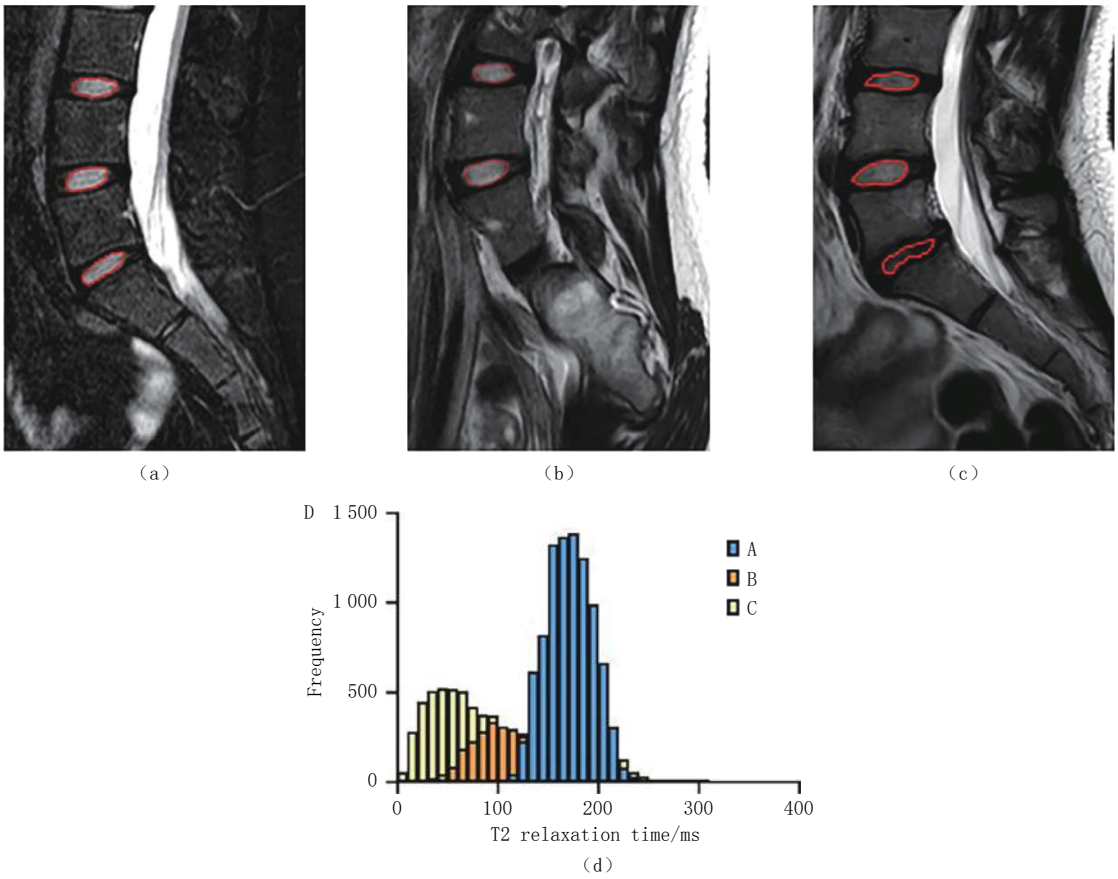

Fig.1 (a) Image of an 18-year-old female volunteer classified as group 0with a mean value of 150.19 ms; (b) Image of a 15-year-old female AIS patients classified as group 1with a mean value of 139.27 ms; (c) Images of a 17-year-old female AIS patients classified as group 2with a mean value of 93.72 ms; (d) Image of the histogram of the three participants in three different groups

3.4 Intra- and Interobserver Agreements

Good intra- and interobserver agreements (ICC 0.803 ~ 0.916) were verified for all histogram-related parameters (Table 5).

4 Discussion

In this study, we performed T2 texture analysis on the intervertebral discs of adolescent idiopathic scoliosis patients and healthy volunteers to prove the effectiveness and superiority of T2 MRI histogram analysis-derived parameters in distinguishing between patients with scoliosis (with or without intervertebral disc degeneration) and healthy volunteers.

The mean value is the most commonly used basic parameter and represents the average T2 relaxation time within a voxel. In our study, we found that the mean values in group 2 were significantly lower than those in groups 0 and 1. This is likely due to the dependency of intervertebral disc homeostasis on the interactions of the extracellular matrix, cells, and biomechanical stress[18]. In group 2 patients with

Table 4　Receiver operating characteristic curves of histogram parameters in distinguishing different groups

	Parameter	Cut-off	Sensitivity/%	Specificity/%	Accuracy	AUC	*P*
Group 0 vs. Group 1	mean	142.840	28.700	95.000	0.485	0.548	0.380
	standard-deviation	63.500	64.900	80.000	0.694	0.679	< 0.001*
	min	23.000	98.900	57.500	0.865	0.796	< 0.001*
	max	345.000	44.700	87.500	0.574	0.599	0.064
	5th percentile	61.000	73.400	90.000	0.783	0.865	< 0.001*
	10th percentile	70.000	60.600	95.000	0.708	0.823	< 0.001*
	25th percentile	100.000	48.900	95.000	0.626	0.727	< 0.001*
	50th percentile	160.000	38.300	95.000	0.552	0.594	0.072
	75th percentile	199.000	70.200	50.000	0.641	0.530	0.591
	90th percentile	286.000	41.500	80.000	0.529	0.540	0.475
	skewness	−0.300	52.100	100.000	0.664	0.695	< 0.001*
	kurtosis	1.950	48.900	100.000	0.641	0.767	< 0.001*
	entropy	5.450	53.200	90.000	0.641	0.637	0.005*
Group 0 vs. Group 2	mean	139.300	92.900	95.000	0.941	0.954	< 0.001*
	standard-deviation	40.360	78.600	100.0000	0.911	0.879	< 0.001*
	min	9.000	82.100	80.000	0.808	0.809	< 0.001*
	max	194.000	82.100	92.500	0.882	0.901	< 0.001*
	5th percentile	52.000	89.300	95.000	0.926	0.933	< 0.001*
	10th percentile	70.000	92.900	95.000	0.941	0.945	< 0.001*
	25th percentile	92.000	92.900	100.000	0.970	0.955	< 0.001*
	50th percentile	142.000	96.400	95.000	0.955	0.967	< 0.001*
	75th percentile	134.000	85.700	100.000	0.941	0.934	< 0.001*
	90th percentile	168.000	85.700	100.000	0.941	0.921	< 0.001*
	skewness	−0.300	89.300	100.000	0.955	0.937	< 0.001*
	kurtosis	2.480	50.000	70.000	0.617	0.538	0.6111
	entropy	5.020	92.900	90.000	0.911	0.962	< 0.001*
Group 1 vs. Group 2	mean	96.170	85.700	100.000	0.967	0.941	< 0.001*
	Standard-deviation	41.780	82.100	95.700	0.926	0.936	< 0.001*
	min	8.000	78.600	52.100	0.581	0.634	0.042*
	max	182.000	78.600	100.000	0.950	0.929	< 0.001*
	5th percentile	30.000	82.100	86.200	0.852	0.839	< 0.001*
	10th percentile	40.000	82.100	94.700	0.918	0.870	< 0.001*
	25th percentile	69.000	85.700	96.800	0.942	0.929	< 0.001*
	50th percentile	127.000	89.300	95.700	0.942	0.960	< 0.001*
	75th percentile	134.000	85.700	100.000	0.967	0.952	< 0.001*
	90th percentile	168.000	85.700	98.900	0.959	0.936	< 0.001*
	skewness	0.010	75.000	88.300	0.852	0.863	< 0.001*
	kurtosis	2.030	85.700	64.900	0.696	0.750	< 0.001*
	entropy	4.890	82.100	90.400	0.885	0.937	< 0.001*

NOTE: Mean and all percentile values are in units of ms. Mean = mean T2 relaxation time; standard deviation = spread of distribution; min = minimum T2 relaxation time; max = maximum T2 relaxation time; 5th, 10th, 25th, 50th, 75th, and 90th percentiles = *n*th percentile T2 relaxation time of a cumulative histogram; skewness = degree of histogram asymmetry around the mean; kurtosis = measurement of histogram sharpness; entropy = distribution of T2 relaxation time levels over the ROI. AUC: area under the receiver operating characteristic (ROC) curve. *−*P* < 0.05.

intervertebral disc degeneration, this balance was disrupted, and the cells stopped producing proteoglycans, which led to a decrease in hydrostatic pressure and an increase in the shear forces on the cells[19-24]. The increased shear forces further decreased proteoglycan production, leading to further degeneration and dehydration of the intervertebral disc[18], consistent with the results of John et al[25] and Zhang et al[9]. The results of the Spearman correlation analysis indicated that the mean value was significantly negatively

correlated from group 0 to group 2, indicating that the T2 relaxation time of the intervertebral discs from group 0 to group 2 showed a downward trend. We hypothesized that the intervertebral discs of group 1 patients had undergone slight histological degeneration, as it was difficult to differentiate with the naked eye the micro differences of the intervertebral discs on conventional images (T2-weighted image) between group 0 and group 1.

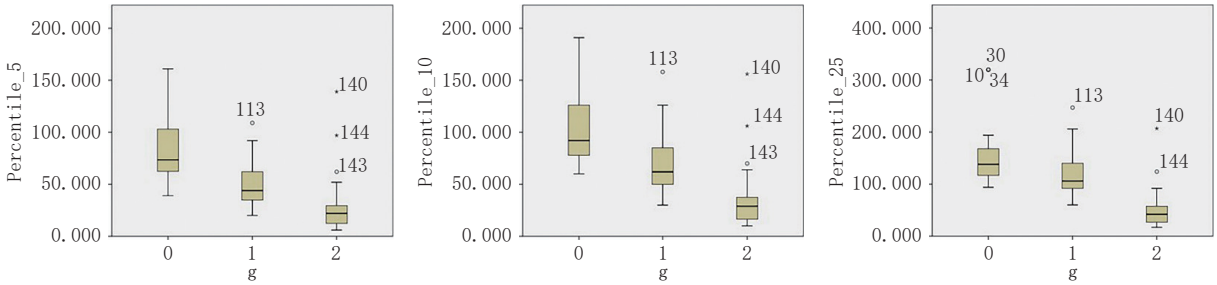

Fig.2 Boxplots of the 5th, 10th, and 25th percentiles. The three parameters can distinguish the differences between the three groups and have a strong negative correlation with g (r = –0.665, –0.652, –0.610)

Table 5 Intra- and Interobserver Agreement of All Parameters

Parameter	Intraobserver agreement		Interobserver agreement		*P*
	ICC	95% CI	ICC	95% CI	
mean	0.852	0.804, 0.890	0.819	0.761, 0.864	< 0.001
standard deviation	0.869	0.826, 0.902	0.836	0.783, 0.877	< 0.001
min	0.856	0.808, 0.892	0.806	0.745, 0.854	< 0.001
max	0.881	0.841, 0.911	0.838	0.785, 0.879	< 0.001
percentile 5	0.846	0.796, 0.885	0.809	0.748, 0.856	< 0.001
percentile 10	0.866	0.822, 0.900	0.830	0.775, 0.872	< 0.001
percentile 25	0.869	0.826, 0.902	0.810	0.749, 0.857	< 0.001
percentile 50	0.900	0.865, 0.925	0.882	0.842, 0.912	< 0.001
percentile 75	0.874	0.832, 0.906	0.836	0.783, 0.877	< 0.001
percentile 90	0.900	0.865, 0.925	0.882	0.842, 0.912	< 0.001
skewness	0.916	0.887, 0.938	0.899	0.865, 0.925	< 0.001
kurtosis	0.887	0.849, 0.916	0.817	0.759, 0.863	< 0.001
entropy	0.828	0.773, 0.871	0.803	0.741, 0.852	< 0.001

NOTE: mean and all percentile values are in units of ms. Mean, mean T2 relaxation time; standard deviation, spread of distribution; min, minimum T2 relaxation time; max, maximum T2 relaxation time; the 5th, 10th, 25th, 50th, 75th, and 90th percentiles, *n*th percentile T2 relaxation time of a cumulative histogram; skewness, histogram asymmetry degree around the mean; kurtosis, measurement of the histogram sharpness; entropy the distribution of T2 relaxation time levels over the ROI. Abbreviations: ICC, intraclass correlation coefficient; CI, confidence interval. *-P < 0.05.

Our results showed that when distinguishing the differences between the three groups, the smaller percentiles (i.e., 5th, 10th, and 25th percentiles) showed better performance and were strongly negatively correlated from group 0 to group 2. The smaller the percentile value, the higher the correlation from group 0 to group 2. Among them, the 5th percentile not only had the highest correlation from group 0 to group 2, but also exhibited the highest efficiency in distinguishing between groups 1 and 0 (AUC = 0.865). The mean value between group 1 and group 0 was not significantly different, which could be due to the superiority of the histogram analysis itself. Through the analysis of each pixel in the histogram, it was found that the slight T2 relaxation time changed owing to the slight degeneration of each pixel and the value of the degraded pixel decreased, which induced more significant changes in the smaller percentile values and better reflected the difference between the two groups. The limitation of the mean value may be because it is the average value of the T2 relaxation time of all voxel points, which cannot reflect the change in each pixel and masks

subtle but important differences between pixels.

Our results showed that the minimum value differed significantly between the three groups, especially in the evaluation of group 0 and group 2 and between group 0 and group 1. The maximum value differed significantly in the evaluation of groups 0 and 2 and between groups 1 and 2; both were significantly negatively correlated from group 0 to group 2. The difference in the results between the maximum and minimum values between the different groups may be due to the following: in groups 0 and 1, some of the pixels of the patients in group 1 underwent slight degeneration, and the T2 relaxation time of the degenerated intervertebral disc was reduced; therefore, among the pixels of the intervertebral disc in group 1, the minimum T2 relaxation time value decreased. However, most of the pixels did not undergo a significant degeneration; therefore, the decrease in the min value changed significantly between the two groups. This is consistent with the smaller percentiles having better efficacy in distinguishing patients in groups 0 and 1. In contrast, the significant reduction in the maximum value in group 2 indicates that the intervertebral discs in group 2 underwent extensive degeneration, generally reducing the T2 relaxation time of the intervertebral disc pixels, while the undegraded pixels in group 1 maintained a higher maximum value, which makes the maximum value better in distinguishing between groups 2 and 1.

Standard deviation is a parameter that reflects the spread of the distribution, entropy reflects the distribution pattern of pixels, and irregularity can be used to measure texture. The higher the entropy value, the more random the grey distribution and stronger the heterogeneity; skewness is a measure of the asymmetry of the distribution, and the greater the absolute value, the greater the asymmetry from the normal distribution[26]. We found that the standard deviation, entropy, and absolute values of skewness showed downward trends in groups 0 to 2, and the histograms shifted to the left and were more symmetrical and gradual in patients in groups 0 to 2. This also shows that as the intervertebral discs from groups to 0 to 2 progressively degenerate, the variability between pixels is reduced, symmetry is increased, and the state of the nucleus pulposus is more uniform, less heterogeneous, and anisotropic, which is in agreement with the results of Antoniou et al[27].

Our study had some limitations. First, owing to ethical issues in human research, the pathological results of patients with AIS and the volunteers could not be obtained. Second, this was a cross-sectional study, and the role of histogram parameters in long-term follow-up and prognostic prediction remains unclear. Third, this study only examined changes in the nucleus pulposus and did not include the annulus fibrosus. These limitations require further investigation.

In conclusion, texture analysis can be used to assess early degenerative changes in the intervertebral discs of patients with AIS that are invisible to the naked eye, especially in the smaller percentiles (i.e., 5th, 10th, and 25th percentiles), which can sensitively assess subtle changes in the intervertebral disc.

参考文献

[1] JANICKI J A, ALMAN B. Scoliosis: Review of diagnosis and treatment[J]. Paediatrics and Child Health, 2007, 12(9): 771-776.

[2] KEENAN B E, IZATT M T, ASKIN G N, et al. Sequential magnetic resonance imaging reveals individual level deformities of vertebrae and discs in the growing scoliotic spine[J]. Spine Deformity, 2017, 5(3): 197-207.

[3] NOHARA A, KAWAKAMI N, TSUJI T, et al. Intervertebral disc degeneration during postoperative follow-up more than 10 years after corrective surgery in idiopathic scoliosis: Comparison between patients with and without surgery[J]. Spine, 2018, 43(4): 255-261.

[4] PFIRRMANN C W, METZDORF A, ZANETTI M, et al. Magnetic resonance classification of lumbar intervertebral disc degeneration[J]. Spine, 2001, 26(17): 1873-1878.

[5] MODIC M T, MASARYK T J, ROSS J S, et al. Imaging of degenerative disk disease[J]. Radiology, 1988, 168(1): 177-186.

[6] BLANQUER S B, GRIJPMA D W, POOT A A. Delivery systems for the treatment of degenerated intervertebral discs[J]. Advanced Drug Delivery Reviews, 2015, 84: 172-187.

[7] OROZCO L, SOLER R, MORERA C, et al. Intervertebral disc repair by autologous mesenchymal bone marrow cells: A

pilot study[J]. Transplantation, 2011, 92(7): 822-828.
[8] BEATTIE P F, MORGAN P S, PETERS D. Diffusion-weighted magnetic resonance imaging of normal and degenerative lumbar intervertebral discs: A new method to potentially quantify the physiologic effect of physical therapy intervention[J]. Journal of Orthopaedic & Sports Physical Therapy, 2008, 38(2): 42-49.
[9] ZHANG W, MA X, WANG Y, et al. Assessment of apparent diffusion coefficient in lumbar intervertebral disc degeneration[J]. European Spine Journal, 2014, 23(9): 1830-1836.
[10] YTRE-HAUGE S, DYBVIK J A, LUNDERVOLD A, et al. Preoperative tumor texture analysis on MRI predicts high-risk disease and reduced survival in endometrial cancer[J]. Journal of Magnetic Resonance Imaging, 2018, 48(6): 1637-1647.
[11] SALA E, MEMA E, HIMOTO Y, et al. Unravelling tumour heterogeneity using next-generation imaging: Radiomics, radiogenomics, and habitat imaging[J]. Clinical Radiology, 2017, 72(1): 3-10. DOI:10.1016/j.crad.2016.09.013.
[12] PANCHMATIA J R, ISAAC A, MUTHUKUMAR T, et al. The 10 key steps for radiographic analysis of adolescent idiopathic scoliosis[J]. Clinical Radiology, 2015, 70(3): 235-242.
[13] STUDER D. Clinical investigation and imaging[J]. Journal of Childrens Orthopaedics, 2013, 7(1): 29-35.
[14] WANG D, WANG S, GAO Y, et al. Diffusion tensor imaging of lumbar vertebras in female adolescent idiopathic scoliosis: Initial findings[J]. Journal of Computer Assisted Tomography, 2018, 42(2): 317-322.
[15] SIEMIONOW K, AN H, MASUDA K, et al. The effects of age, sex, ethnicity, and spinal level on the rate of intervertebral disc degeneration: A review of 1712 intervertebral discs[J]. Spine, 2011, 36(17): 1333-1339.
[16] LIU S, SHI H, JI C, et al. Preoperative CT texture analysis of gastric cancer: Correlations with postoperative TNM staging[J]. Clinical Radiology, 2018, 73(8): 756.e1-756.e9.
[17] LIU S, LIU S, JI C, et al. Application of CT texture analysis in predicting histopathological characteristics of gastric cancers[J]. European Radiology, 2017, 27(12): 4951-4959.
[18] VERGROESEN P P, KINGMA I, EMANUEL K S, et al. Mechanics and biology in intervertebral disc degeneration: A vicious circle[J]. Osteoarthritis and Cartilage, 2015, 23(7): 1057-1070.
[19] WEILER C, NERLICH A G, ZIPPERER J, et al. 2002 SSE Award Competition in Basic Science: Expression of major matrix metalloproteinases is associated with intervertebral disc degradation and resorption[J]. European Spine Journal, 2002, 11(4): 308-320.
[20] ANTONIOU J, STEFFEN T, NELSON F, et al. The human lumbar intervertebral disc: Evidence for changes in the biosynthesis and denaturation of the extracellular matrix with growth, maturation, ageing, and degeneration[J]. Journal of Clinical Investigation, 1996, 98(4): 996-1003.
[21] ZHANG Z, CHAN Q, ANTHONY M P, et al. Age-related diffusion patterns in human lumbar intervertebral discs: A pilot study in asymptomatic subjects[J]. Magnetic Resonance Imaging, 2012, 30(2): 181-188.
[22] CARTER D R, WONG M. Modelling cartilage mechanobiology[J]. Philosophical Transactions of the Royal Society B-Biological Sciences, 2003, 358(1437): 1461-1471.
[23] SZTROLOVICS R, ALINI M, ROUGHLEY P J, et al. Aggrecan degradation in human intervertebral disc and articular cartilage[J]. Biochemical Journal, 1997, 326(Pt 1): 235-241.
[24] SMITH R L, CARTER D R, SCHURMAN D J. Pressure and shear differentially alter human articular chondrocyte metabolism: A review[J]. Clinical Orthopaedics and Related Research, 2004, (427Suppl): S89-95.
[25] ANTONIOU J, DEMERS C N, BEAUDOIN G, et al. Apparent diffusion coefficient of intervertebral discs related to matrix composition and integrity[J]. Magnetic Resonance Imaging, 2004, 22(7): 963-972. DOI:10.1016/j.mri.2004.02.011.
[26] ALOBAIDLI S, MCQUAID S, SOUTH C, et al. The role of texture analysis in imaging as an outcome predictor and potential tool in radiotherapy treatment planning[J]. British Journal of Radiology, 2014, 87(1042): 20140369.
[27] ANTONIOU J, EPURE L M, MICHALEK A J, et al. Analysis of quantitative magnetic resonance imaging and biomechanical parameters on human discs with different grades of degeneration[J]. Journal of Magnetic Resonance Imaging, 2013, 38(6): 1402-1414.

基于 MRI T2 加权成像纹理分析评估青少年脊柱侧弯患者椎间盘退变的可行性研究

王凤仙[a]，王守丰[b]，常莹[a]，周晋[a]，陈静[a]，周正扬[a✉]，王冬梅[2✉]

1. 南京大学医学院附属南京鼓楼医院 a）放射科；b）骨科，南京 210008
2. 上海中医药大学附属上海市中医医院放射科，上海 200071

摘要：目的：探讨 MRI T2 加权成像纹理分析在青少年脊柱侧弯患者椎间盘退变中的应用价值。材料和方法：从 2016 年 10 月至 2020 年 3 月，前瞻性纳入 122 例 AIS 患者和 40 名志愿者行 3.0T 磁共振成像（MRI）检查并得到患者图像 MRI 纹理参数值：① 平均值，② 标准差，③ 最大值，④ 最小值，⑤ 第 5、10、25、50、75 和 90 百分位数，⑥ 偏度，⑦ 峰度，⑧ 熵。采用 Pfirrmann 评分对所有参与者的椎间盘进行评估并分组，AIS 患者中，评分为 Pm I 的患者纳入 1 组，其余患者纳入 2 组，志愿者纳入 0 组；分析组间差异性和相关性。结果：2 组的均值、标准差、最大值、熵和第 5、10、25、50、75、90 百分位均显著低于 1 组和 0 组；2 组 min 显著低于 0 组；2 组偏度显著高于 1 组和 0 组；2 组峰度显著低于 1 组；1 组偏度显著高于 0 组，1 组标准差、最小值、峰度和第 5、10、25、50 百分位显著低于 0 组。结论：纹理分析可用于评估 AIS 患者椎间盘早期退行性改变，且优于常规 MRI T2 加权成像。

关键词：MRI；纹理分析；青少年脊柱侧弯；椎间盘退变

作者简介：王凤仙，女，南京大学医学院附属南京鼓楼医院住院医师，主要从事骨肌影像学的诊断及功能成像在临床上应用研究，E-mail：279782670@qq.com；周正扬✉，男，南京大学医学院附属南京鼓楼医院主任医师、教授，主要研究方向为多排 CT 与 MR 的基础和临床应用研究和磁共振淋巴造影对肿瘤转移性淋巴结定性诊断的基础和临床研究，E-mail：zyzhou@nju.edu.cn；王冬梅✉，女，上海中医药大学附属上海市中医院主任医师，主要骨肌影像学的诊断和成像新技术的开发与临床应用研究，E-mail：dongmeiwang9320@163.com。